Desalination and Water Treatment
www.deswater.com
doi: 10.5004/dwt.2018.22977

133 (2018) 153–166
November

Process optimization of potassium hydroxide activated carbon from carob shell biomass and heavy metals removal ability using Box–Behnken design

M. Farnane[a], A. Machrouhi[a], A. Elhalil[a], H. Tounsadi[a,b,*], M. Abdennouri[a], S. Qourzal[c], N. Barka[a]

[a]*Laboratoire des Sciences des Matériaux, des Milieux et de la Modélisation (LS3M), FPK, Univ Hassan 1, B.P.: 145, 25000 Khouribga, Morocco, Tel. +212 645 20 85 64; Fax: +212 523 49 03 54; emails: hananetounsadi@gmail.com (H. Tounsadi), Farnane.meryem@gmail.com (M. Farnane), machrouhi.aicha90@gmail.com (A. Machrouhi), elhalil.alaaeddine@gmail.com (A. Elhalil), abdennourimohamed@yahoo.fr (M. Abdennouri), barkanoureddine@yahoo.fr (N. Barka)*
[b]*Faculté des Sciences Dhar Elmehraz, Laboratoire d'Ingénierie, d'Electrochimie, de Modélisation et d'Environnement, Université Sidi Mohamed Ben Abdellah, Fès, Morocco*
[c]*Equipe de Catalyse et Environnement, Département de Chimie, Faculté des Sciences, Université Ibn Zohr, B.P. 8106 Cité Dakhla, Agadir, Morocco, email: samir_qourzal@yahoo.fr*

Received 18 January 2018; Accepted 12 August 2018

ABSTRACT

This work investigated the utilization of carob shell biomass as a precursor for the preparation of activated carbons by potassium hydroxide activation and their use for heavy metals removal from aqueous solutions. Experimental design approach was adopted for the optimization of preparation conditions and cobalt and cadmium removal efficiency. A Box–Behnken surface statistical design with three factors and three-level combining with response surface modeling and quadratic programming was employed for maximizing cadmium and cobalt ions removal from aqueous solution. Three different factors including impregnation ratio, activation time, and activation temperature were used. Experimental results showed that the activation temperature was the most significant factor with a negative impact for iodine number, methylene blue index, and the removal of cadmium and cobalt ions. Furthermore, the impregnation ratio showed a negative impact for iodine number and methylene blue index. The activation time presented a positive effect for methylene blue index. Moreover, the interaction between activation time and activation temperature had a negative impact for cadmium and cobalt ions removal. Optimal conditions for cadmium removal were achieved with an impregnation ratio of 0.3 g/g, activation time of 1.5 h, and an activation temperature at 400°C. Sorption capacities were determined with equilibrium isotherms. Greater sorption efficiencies acquiring via Langmuir isotherm model were 90.58 mg/g for cadmium removal and 77.24 mg/g for cobalt sorption. These major values were obtained for the activated carbons prepared with an impregnation ratio of 0.3 g/g, activation time of 1.5 h and an activation temperature at 400°C and an impregnation ratio of 0.1 g/g, activation time of 1.5 h and an activation temperature at 400°C, respectively.

Keywords: Carob shells biomass; Activated carbon; Cadmium; Cobalt; Potassium hydroxide; Box–Behnken design.

1. Introduction

The economy of the water is very necessary to save the planet and to the future of humanity. With the growth of humanity, science, and technology, the world achieved to new horizons but the cost that we will pay in the near future will surely be too high. Among the effect of this rapid growth is the environmental mess with a big pollution problem. The demand for water has increased tremendously with the consumption of agricultural, industrial,

* Corresponding author.

and domestic sectors and this resulted in the generation of large amounts of wastewater containing many pollutants [1]. Among the most dangerous pollutants, heavy metals may constitute risk factors for our health and nuisance to our environment [2]. Therefore, it is necessary to limit these pollutants as far as possible by establishing a suitable treatment process [3]. There are several physical, chemical, and biological methods to treat polluted effluents such as: filtration [4], solvent extraction [5], electrochemical treatment [6], chemical precipitation [7], ion exchange [8], reverse osmosis [9], and adsorption [10,11]. Among these processes, adsorption is one of the most favorable methods for the removal of heavy metals due to its effectiveness and its simplicity in using [12,13]. The principle of adsorption treatment is to trap metals with a solid adsorbent material. In the literature, several solid materials including zeolite, clay [14], nanotubes [15], graphene oxide [16], nanocomposites [17], sericite [18], biomasses, and activated carbon were used in wastewater treatment processes. Because of their extensive porous structure, their high surface area and high adsorption capacity, the activated carbon is mostly used for treating wastewaters [19]. In the recent years, many low-cost materials which are available locally and biodegradable have been widely used in the production of activated carbons. To preserve the environment natural materials including apple shell [20], olive pits [21], flamboyant pods [22], apricot stones [23], coconut shell [24], hazelnut shell [25], rice straw [26], *Diplotaxis harra* [27], and *Glebionis coronaria* L. [28] have been developed as precursors for the production of activated carbon.

In this way, chemical activation processes is widely used due to its lower activation temperature (usually around 400°C–600°C) and its high product yield as compared with physical process which requires high temperatures (>850°C). Well-known chemical agents, $ZnCl_2$, H_3PO_4, H_2SO_4, HNO_3, H_2O_2, $KMnO_4$, NaOH, KOH, and K_2CO_3, are used to activate carbons, resulting in a high surface area and appropriate porous structure. Among these chemical activating agents, it has been reported that KOH activation shows improvement in specific surface area and capacitive performance [29]. In order to optimize experimental conditions, experimental designs have been used to control the different factors which influence and interfere in the preparation and the treatment of results [30–32].

This study focused on the potassium hydroxide activation of de-oiled carob shells obtained after hydrodistillation. Preparation conditions, cadmium and cobalt ions removal were optimized using Box–Behnken experimental design. Factors included in this model were the activation temperature, activation time, and impregnation ratio. Four responses were analyzed, which are iodine number (IN), methylene blue index (MB index), cadmium and cobalt ions removal (Cd(II), Co(II)). The activated carbon (AC) produced at the optimal conditions was characterized by the Fourier transform infrared spectroscopy (FTIR) and the point of zero charge (pH_{PZC}). Functional groups were quantified by Boehm titration. As well, for the optimized activated carbons, the equilibrium data of heavy metal ions sorption were analyzed by Langmuir and Freundlich isotherm models.

2. Material and methods

2.1. Materials

All the chemicals used in this study were of analytical grade. $Cd(NO_3)_2{\cdot}4H_2O$ (98%), $Co(NO_3)_2{\cdot}6H_2O$ (98%), potassium hydroxide (KOH) (98%), NaCl (99.5%), iodine (I_2), sodium thiosulfate ($Na_2S_2O_3{\cdot}5H_2O$), Na_2CO_3, $NaHCO_3$, and HCl (37%) were purchased from Sigma-Aldrich (St. Louis, MO, USA). HNO_3 (65%) was provided from Scharlau (Scharlab, Barcelona, Spain). NaOH was from Merck (Darmstadt, Germany), potassium iodide (KI) was obtained from Pharmac (St. new Pharmac, Casablanca, Morocco) and MB was purchased from Panreac (Quimica SLU - Castellar Del Valles, Spain).

2.2. Preparation of activated carbons

The carob shells were collected from the region of Khenifra in Morocco. First, they were washed several times with distilled water to remove impurities and then crushed and sieved to the desired particle sizes 1–2 mm. Thereafter, these shells were hydrodistilled in clevenger apparatus to extract essential oils. The residual biomass was used for the preparation of activated carbon. This result product was impregnated with potassium hydroxide to carbon ratio (g KOH/g carbon) of 0.1–0.3 g/g. At first, the residual biomass and KOH were mixed in 50 mL of distilled water, and then the mixture is shaken at 500 rpm for 1 h at room temperature. Second, the impregnated biomass was thermally activated in a furnace at 400°C–600°C during activation time 1–2 h under nitrogen flux. The obtained activated carbons were washed with hot distilled water until neutral pH. Therefore they were dried at 105°C, ground and sieved at a size lower than 125 μm using a normalized sieve. The obtained activated carbons were kept in hermetic bottle for subsequent use.

2.3. Characterization

2.3.1. Surface groups and pH_{PZC}

Functional groups on the activated carbons surface were identified by using a Scotech-SP-1 spectrophotometer in the range of 4,000–400 cm^{-1}. Samples were prepared in KBr disks. Boehm titrations [33] were used for determining acidic and basic groups. In this method, about 0.1 g of each sample was mixed with 50 mL of 0.01 M aqueous reactant solution (NaOH, Na_2CO_3, $NaHCO_3$, or HCl). The mixtures were stirred at 500 rpm for 24 h at room temperature. Then, the suspensions were filtrated by a 0.45 μm membrane filter. To determine the oxygenated groups content, back titrations of the filtrate (10 mL) were achieved with standard 0.01 M HCl solution. Basic groups contents were also determined by back titration of the filtrate with 0.01 M NaOH solution. pH_{PZC} of different carbons were determined by "mass titration method" [34]. Thus, 0.05 g of each biosorbents was added to 50 mL of solution of NaCl (0.01 M). The initial pH of the solution was adjusted to defined values from 2.0 to 12.0 using HNO_3 and NaOH (1 M) solutions. The solutions were stirred for 6 h and the final pH was measured and plotted

against the initial pH using a sensION + PH31 pH meter. The pH_{PZC} was determined at $pH_{final} = pH_{initial}$.

2.3.2. Iodine number

The IN is a technique employed to determine the adsorption capacity of activated carbons. IN can be used as an approximation for surface area and microporosity of active carbons with good precision. The iodine adsorption was determined using ASTM D4607-94 method. It is a measure of activity level (higher number indicates higher degree of activation), often reported in mg/g (typical range 500–1,200 mg/g). It is a measure of the micropore content of the activated carbon (0–20 Å, or up to 2 nm) by adsorption of iodine from solution. It is equivalent to surface area of carbon between 900 and 1,100 m^2/g [35]. The IN is defined as the amount of iodine adsorbed by 1 g of carbon when the iodine concentration of the filtrate is 0.02 N. So 1 g of each carbon are treated with 10.0 mL of 5% HCl and boiled for 30 s and subsequently cooled. 100 mL of 0.1 N iodine solution was added to the mixture and stirred for 30 min. The resulting solution was filtered and 50 mL of the filtrate was titrated with 0.1 N of sodium thiosulfate using starch as indicator.

2.3.3. Methylene blue index

The MB index is the number of milligrams of MB adsorbed per gram of activated carbon. It gives an idea of the available surface area for micro- and mesoporous adsorbents. To have maximum sorption capacities of MB, the adsorption isotherms were investigated. Stock solution of MB was prepared by dissolving desired weight in distilled water. Sorption experiments were investigated in a series of beakers containing 100 mL by adding 100 mg of each carbon. Sorption equilibrium was established for different MB initial concentration between 20 and 500 mg/L for 12 h at room temperature. Residual concentrations were determined by spectrophotometric method at the wavelength of maximum absorbance of 665 nm.

2.3.4. Heavy metals removal

Metal solutions of cadmium and cobalt ions were prepared by dissolving desired weight of $Cd(NO_3)_2{\cdot}4H_2O$ or $Co(NO_3)_2{\cdot}6H_2O$ in distilled water. Sorption experiments were investigated in a series of beakers containing 50 mL of the metal ions solution with a concentration of 100 mg/L and 50 mg of each activated carbon. The mixtures were stirred for 3 h at 500 rpm. The pH of the solutions was adjusted to 6.50 during the experiment with either 0.1 mol/L of HCl or NaOH and measured by a sensION + PH31 pH meter.

After each sorption experiment, samples were centrifuged at 3,400 rpm for 10 min. Metal ion concentrations were determined using a Perkin-Elmer atomic absorption spectrophotometer (AAnalyst 200). The adsorption capacity of the heavy metals at equilibrium was defined as the amount of adsorbate per gram of adsorbent (in mg/g) and was calculated using following equation:

$$q_e = \frac{\left(C_0 - C_e\right)}{R} \quad (1)$$

where q_e is the adsorbed quantity (mg/g), C_0 is the initial metal concentration (mg/L), C_e is the residual metal concentration (mg/L), and R is the mass of activated carbon per liter of aqueous solution (g/L).

Sorption equilibrium for the optimized activated carbons was investigated for different metal concentrations between 20 and 200 mg/L. The experimental results were correlated to Langmuir and Freundlich isotherm models via nonlinear fitting using Origin 6.0 software.

2.4. Box–Behnken experimental design

The Box–Behnken design is used to optimize the number of experiments to be carried out to possible interactions between parameters studied and their effects on the removal of heavy metals [36]. It is an experimental design combined with response surface modeling and quadratic programming. Three factors were used including, impregnation ratio (X_1 = 0.1, 0.2, and 0.3 g/g), activation time (X_2 = 1, 1.5, and 2 h), and activation temperature (X_3 = 400°C, 500°C, and 600°C). These variables with their respective domain are chosen on the basis of the literature data and preliminary experiments. Each factor was varied at three different levels −1, 0, and +1 signifying low, medium, and high values. A first-order model with all possible interactions was chosen to fit the experimental data (Eq. (2)).

$$Y = \beta_0 + \sum \beta_i X_i + \sum \beta_{ii} X_{i2} + \sum \beta_i X_i^2 + \sum_i \sum_j \beta_{ij} X_i X_j + e_i \quad (2)$$

where β_0 is the constant, β_i the slope or linear effect of the input factor X_i, β_{ij} is the linear by linear interaction effect between the input factor X_i and X_j, β_{ij} is the quadratic effect of input factor X_i.

3. Results and discussion

3.1. Process optimization

3.1.1. Experimental results

Table 1 shows preparation conditions and experimental results for studding responses; IN, MB index, cadmium and cobalt removal. Values of MB index varied between 36.79 and 208.46 mg/g, were indicated a high mesoporosity for almost activated carbon samples. It could be seen that the impregnation ratio had a great influence on the adsorption capacity. For the IN, the high value of 822.5 mg/g was obtained for the carbon activated at 500°C for 2 h with an impregnation ratio of 0.1 g/g. A low impregnation ratio was given a best result. For the removal of cadmium and cobalt ions, it could be seen that, the maximum sorption capacities were 67.69 and 51.64 mg/g, respectively, for the carbon activated at 400°C for 1.5 h with an impregnation ratio of 0.1 g/g and the carbon activated at 400°C for 1.5 h with an impregnation ratio of 0.3 g/g.

In fact, the regression analysis was performed to fit response functions with the experimental data. Values of regression coefficient obtained are presented in Table 2. According to the table, the impregnation ratio presented a negative effect on IN, MB index, and cobalt ions removal and a positive effect on the cadmium ions removal. While, the

Table 1
Factorial experimental design matrix coded, real values and experimental results of the responses

Run	Coded values			Actual values			Responses (mg/g)			
	X_1	X_2	X_3	X_1	X_2	X_3	IN	MB index	Cd(II)	Co(II)
1	−1	0	−1	0.1	1 h 30	400	640.99	177.66	60.80	51.64
2	0	0	0	0.2	1 h 30	500	654.95	215.38	41.96	32.43
3	+1	−1	0	0.3	1 h	500	557.22	56.90	54.36	45.99
4	0	−1	−1	0.2	1 h	400	682.88	154.82	50.23	35.82
5	−1	−1	0	0.1	1 h	500	752.69	201.02	38.28	36.95
6	+1	0	−1	0.3	1 h 30	400	599.11	45.89	67.69	48.81
7	0	0	−1	0.2	1 h 30	400	668.92	185.25	60.80	49.39
8	0	+1	0	0.2	2 h	500	710.08	285.25	43.79	38.07
9	−1	+1	0	0.1	2 h	500	822.50	243.35	36.90	35.25
10	0	+1	+1	0.2	2 h	600	389.67	129.61	31.39	28.47
11	+1	+1	0	0.3	2 h	500	473.44	73.49	41.96	36.94
12	−1	0	+1	0.1	1 h 30	600	417.59	111.78	29.55	30.73
13	0	+1	−1	0.2	2 h	400	724.77	275.13	66.31	40.34
14	0	0	+1	0.2	1 h 30	600	501.37	117.33	28.63	30.73
15	0	−1	+1	0.2	1 h	600	459.48	102.29	37.82	31.30
16	0	−1	0	0.2	1 h	500	780.62	188.91	39.20	45.60
17	+1	0	+1	0.3	1 h 30	600	361.75	73.24	26.79	20.00

Table 2
Values of model coefficients for the four responses

Main coefficients	Y_1	Y_2	Y_3	Y_4
b_0	696.86	232.82	40.83	38.75
b_1	−91.52	−63.06	2.81	−0.47
b_2	−11.24	30.30	0.05	−1.66
b_3	−126.63	−37.21	−16.16	−8.50
b_{12}	−56.24	−12.61	−1.76	−0.58
b_{13}	−3.49	23.31	−2.41	−1.98
b_{23}	−33.12	−28.17	−3.92	−0.08
b_{11}	−62.34	−69.62	0.95	0.78
b_{22}	19.21	−12.13	1.16	−0.61
b_{33}	−139.50	−54.39	4.25	−2.43

activation time had a negative effect on IN and cobalt ions removal and positive effects on the MB index and cadmium ions removal. Whereas, the activation temperature had a negative effect on the IN, the MB index, and both the heavy metals removal. The analysis of the interaction effects showed a significant interaction with a negative impact between impregnation ratio and activation time on the IN (b_{12} = −56.24), and a significant interaction between impregnation ratio and activation temperature on MB index response with a positive effect (b_{13} = 23.31). For the heavy metal ions removal, the interactions of the impregnation ratio showed a significant effect with a positive sign (b_{11} = 0.95 for cadmium removal and b_{11} = 0.78 for cobalt removal).

3.1.2. Analysis of variance

The analysis of variance (ANOVA) is used to determine the significance of the curvature in the responses at a confidence level of 95%. The effect of a factor is defined as the change in response produced by a change in the level of the factor. This is frequently called a main effect because it refers to the primary factors of interest in the experiment. The model and model terms are considered to be significant only when the values of (Prob > *F*) are less than 0.05 and terms with Fisher's statistical test (*F*-test). According to these conditions, several studies were analyzed [37]. The ANOVA assessed the significance fitting of the quadratic model for four responses with results indicated in Table 3. ANOVA results showed that equations adequately represented the actual relationship between each response and significant variables.

3.1.2.1. Iodine number

According to the ANOVA analysis for the IN, significant effects are the impregnation ratio (X_1), activation temperature (X_3), and the interaction between impregnation ratio × impregnation ratio (X_{12}) and activation temperature × activation temperature (X_{32}). These factors and interaction showed a negative effect on the IN. So, IN increased as the impregnation ratio and activation temperature decreased. In contrast, an increase in the micropores was occurred for low level of the impregnation ratio (0.1 g/g) and the activation temperature of 400°C. The final equation in terms of coded factors was described as follows:

$$Y_1 = 716.07 - 91.53X_1 - 9.40X_2 - 126.63X_3 - 56.24X_1X_2 - 33.12X_2X_3 - 66.19X_1^2 - 147.20X_3^2 \quad (3)$$

3.1.2.2. Methylene blue index

For the MB index, most significant effects are impregnation ratio, activation time, activation temperature, and the interaction of impregnation ratio × impregnation ratio

Table 3
Analysis of variance for the four responses

Source	Sum of squares	Df	Mean square	*F*-Value	p-Value Prob > *F*	
			Iodine number			
Model	303,411.56	7	43,344.51	14.12	0.0003	Significant
X_1	62,398.40	1	62,398.39	20.32	0.0015	
X_2	925.17	1	925.17	0.30	0.5964	
X_3	141,731.16	1	141,731.16	46.16	<0.0001	
X_1X_2	13,663.35	1	13,663.35	4.45	0.0641	
X_2X_3	4,809.78	1	4,809.78	1.47	0.2423	
X_1^2	17,955.46	1	17,955.46	5.85	0.0387	
X_3^2	85,365.58	1	85,365.58	27.80	0.0005	
Residual	27,633.47	9	3,070.39			
Cor total	331,045.03	16				
					$R^2 = 0.9165$; $R^2_{adj} = 0.8516$	
			Methylene blue index			
Model	81,088.77	7	11,584.11	12.93	0.0005	Significant
X_1	29,317.10	1	29,317.10	32.73	0.0003	
X_2	8,897.46	1	8,897.46	9.93	0.0117	
X_3	12,238.20	1	12,238.20	13.66	0.0049	
X_1X_3	2,172.96	1	2,172.96	2.43	0.1538	
X_2X_3	3,478.51	1	3,478.51	3.88	0.0802	
X_1^2	18,499.42	1	18,499.42	20.65	0.0014	
X_3^2	9,663.53	1	9,663.53	10.79	0.0095	
Residual	8,061.20	9	895.69			
Cor total	89,149.96	16				
					$R^2 = 0.9165$; $R^2_{adj} = 0.8516$	
			Cd(II) removal			
Model	2,470.40	6	411.73	11.83	0.0005	Significant
X_1	79.82	1	79.82	2.29	0.1608	
X_2	0.19	1	0.19	0.01	0.9430	
X_3	2,292.62	1	2,292.62	65.89	<0.0001	
X_1X_3	23.28	1	23.28	0.67	0.4324	
X_2X_3	67.31	1	67.31	1.93	0.1944	
X_1^2	0.02	1	0.02	0.001	0.9891	
Residual	347.92	10	34.79			
Cor total	2,818.33	16				
					$R^2 = 0.8765$; $R^2_{adj} = 0.8025$	
			Co(II) removal			
Model	769.12	6	128.17	3.22	0.0499	Significant
X_1	1.00	1	1.00	0.03	0.8772	
X_2	25.69	1	25.69	0.64	0.4406	
X_3	637.96	1	637.96	16.02	0.0025	
X_1X_3	15.60	1	15.60	0.39	0.5454	
X_2X_3	0.03	1	0.03	0.001	0.9798	
X_1^2	6.92	1	6.92	0.17	0.6856	
Residual	398.34	10	39.83			
Cor total	1,167.36	16				
					$R^2 = 0.6588$; $R^2_{adj} = 0.4540$	

and the activation temperature × activation temperature. The impregnation ratio, activation temperature, and the interactions X_{12} and X_{32} showed a negative effect on the MB index response. In contrast, activation time had a positive effect. Therefore, the MB index increased when the activation time was in the high level (2 h). Therefore, the preparation of an activated carbon with a high mesoporosity suggested to use a low impregnation ratio (0.1 g/g) and a less activation temperature (400°C).

$$Y_2 = 220.69 - 60.54X_1 + 29.14X_2 - 37.21X_3 + 23.31X_1X_3 - 28.17X_2X_3 - 67.19X_1^2 - 49X_3^2 \quad (4)$$

3.1.2.3. Heavy metals removal

Basis on the ANOVA analysis, both responses of cadmium and cobalt ions removal showed that the most significant factor was the activation temperature (X_3). It had a negative impact on cadmium and cobalt ions removal. In fact, the elimination efficiency of heavy metals increased if the activation temperature was 400°C. Therefore, it was observed that the models of cadmium and cobalt ions removal are similar. This result suggested that the cadmium and cobalt ions were adsorbed in the same kind of pores.

$$Y_3 = 44.44 + 3.16X_1 - 0.13X_2 - 16.11X_3 - 2.41X_1X_3 - 3.92X_2X_3 + 0.07X_1^2 \quad (5)$$

$$Y_4 = 36.70 - 0.35X_1 - 1.55X_2 - 8.50X_3 - 1.98X_1X_3 - 0.08X_2X_3 + 1.28X_1^2 \quad (6)$$

3.1.3. Diagnostic model

Statistical actual and predicted values for testing significant effects of regression coefficients for proposed models as diagnostic are presented in Table 4. Values obtained by the model (Y predicted) are compared with those of experimental data (Y experimental). Correlations between theoretical and experimental responses, calculated by the model, were satisfactory. Therefore, the "R^2" were in reasonable agreement with the "R^2_{Adj}". Furthermore, "R^2" were greater than "R^2_{Adj}". It can be seen that more than 95% of these responses can be well predicted by these models, indicating that terms which were considered in proposed models were significant enough to make acceptable predictions. The Model F-value of the IN, MB index, cadmium and cobalt removal were including 14.12, 12.93, 11.83, and 3.22, respectively, implies that models are significant. There was only a 0.03% chance for iodine, 0.05% chance for the MB index and the cadmium removal, and 5.00% chance for the cobalt removal. Indeed, the high value of F-ratio confirms the significance of proposed models.

3.1.4. Response surface analysis

The 3D response surface plot obtained from statistical processes for different combinations and the desirability function based on the design are depicted in Figs. 1 and 2. For the IN, the most significant interactions were activation time/impregnation ratio and activation temperature/activation time. For MB index and the removal of cadmium and cobalt, there were the same as significant interactions including activation temperature/impregnation ratio and activation temperature/activation time.

3.1.4.1. Iodine number

Fig. 1(a) shows that the IN increased with decreasing of the impregnation ratio and the activation time varied between 1 and 2 h, when activation temperature was fixed

Table 4
Factorial design matrix of four variables along with experimental and predicted responses for IN, MB index, Cd(II), and Co(II)

Run	IN			MB index			Cd(II)			Co(II)		
	Actual	Predicted	Residual	Actual	Predicted	Residual	Actual	Predicted	Residual	Actual	Predicted	Residual
1	641.0	688.9	−47.9	177.7	202.1	−24.5	60.8	53.5	7.3	51.6	45.4	6.2
2	655.0	719.8	−64.9	215.4	209.0	6.3	42.0	44.5	−2.5	32.4	37.3	−4.9
3	557.2	623.9	−66.8	56.9	63.8	−6.9	54.4	47.8	6.6	46.0	39.2	6.8
4	682.9	671.8	11.1	154.8	151.1	3.7	50.2	56.8	−6.5	35.8	46.7	−10.8
5	752.7	694.6	58.1	201.0	184.9	16.1	38.3	41.5	−3.2	36.9	39.9	−2.9
6	599.1	550.8	48.3	45.89	34.4	11.5	67.7	64.7	3.0	48.8	48.7	0.1
7	668.9	686.0	−17.1	185.3	185.5	−0.2	60.8	59.0	1.8	49.4	45.8	3.6
8	710.1	706.7	3.4	285.4	249.8	35.6	43.8	44.3	−0.5	38.1	35.1	2.9
9	822.5	788.3	34.2	243.4	243.2	0.17	36.9	41.2	−4.3	35.3	36.8	−1.5
10	389.7	399.7	−10.1	129.6	135.0	−5.3	31.4	24.3	7.1	28.5	26.6	1.9
11	473.4	492.7	−19.3	73.5	122.1	−48.6	42.0	47.5	−5.6	37.0	36.07	0.9
12	417.6	462.1	−44.5	111.8	103.6	8.2	29.6	29.3	0.3	30.7	32.5	−1.7
13	724.8	719.2	5.53	275.1	265.7	9.4	66.3	64.3	2.0	40.3	43.7	−3.4
14	501.4	459.3	42.1	117.3	133.6	−16.2	28.6	30.0	−1.3	30.7	28.9	1.9
15	459.5	484.8	−25.3	102.3	133.0	−30.7	37.8	32.4	5.4	31.3	29.8	1.5
16	780.6	725.5	55.2	188.9	191.6	−2.6	39.2	44.6	−5.4	45.6	38.3	7.3
17	361.8	324.0	37.7	73.2	29.2	44.1	26.8	30.1	−4.0	20	27.8	−7.8

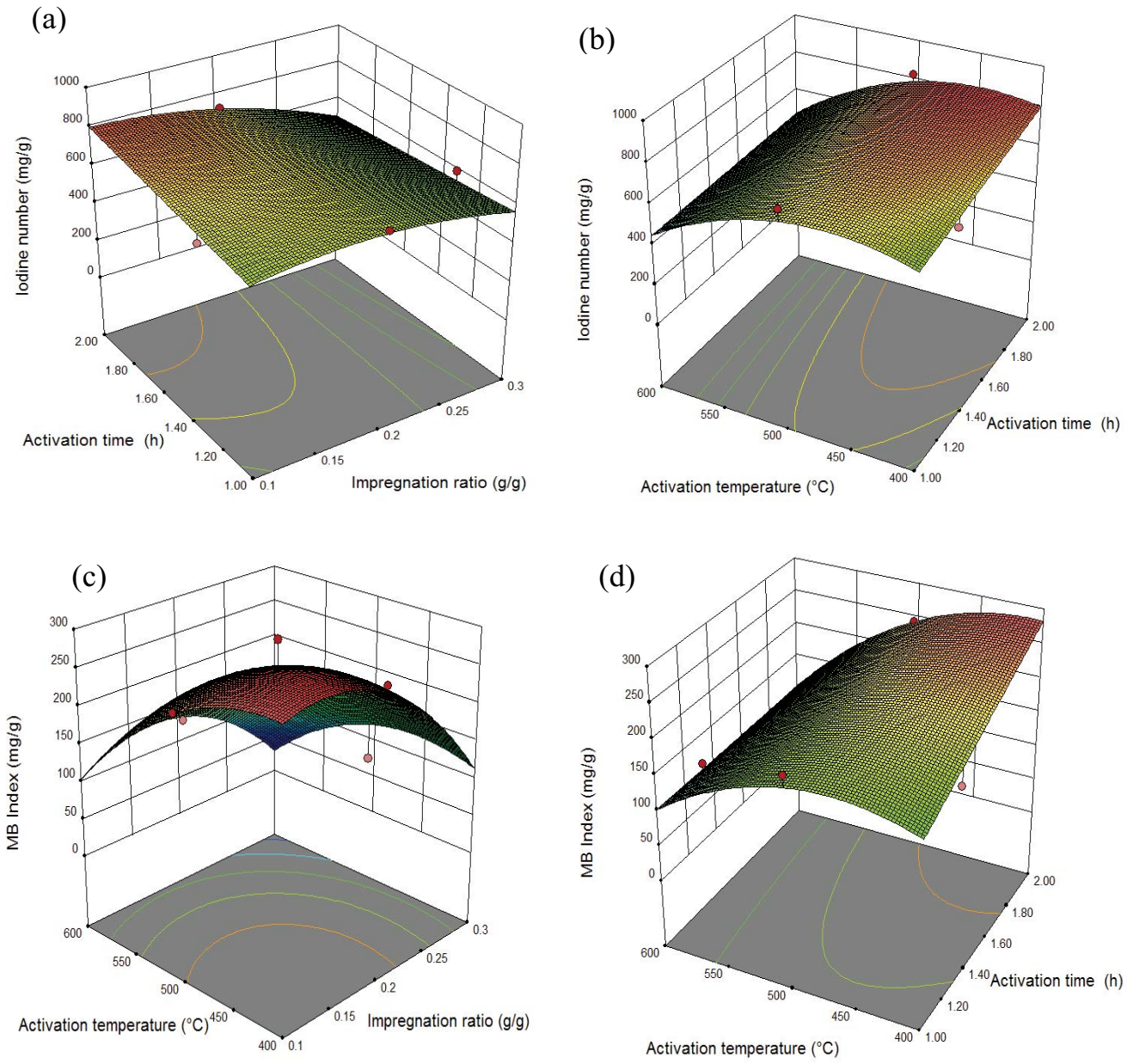

Fig. 1. Surface response plot for iodine number (a, b) and methylene blue index (c, d).

at 400°C. The maximal IN was observed at 0.1 g/g whatever the activation time is. Fig. 1(b) indicated that the IN increased with decreasing of the activation temperature and the activation time varied between 1 and 2 h, when impregnation ratio is fixed at 0.1 g/g. A maximal value of IN was observed at 400°C whatever the activation time is.

3.1.4.2. Methylene blue index

According to Fig. 1(c), we can see that the MB index increased with decreasing of activation temperature and impregnation ratio. A maximal MB index was observed at activation temperature of 400°C, impregnation ratio of 0.1 g/g with the activation time 2 h. Fig. 1(d) shows that the MB index increased with decreasing of the activation temperature when the activation time increased. So a maximal MB index was obtained at 400°C regardless of the activation time.

3.1.4.3. Heavy metals removal

Figs. 2(a) and (c) indicate that the elimination of Cd(II) and Co(II) are influenced by same factors and that the adsorption of these two metals increased with decreasing of the activation temperature when the impregnation ratio varied between 0.1 and 0.3 g/g, with a fixed activation time at 1 h for removal of Cd(II) and at 2 h for removal of Co(II). For that, a great value of metal removal was obtained at activation

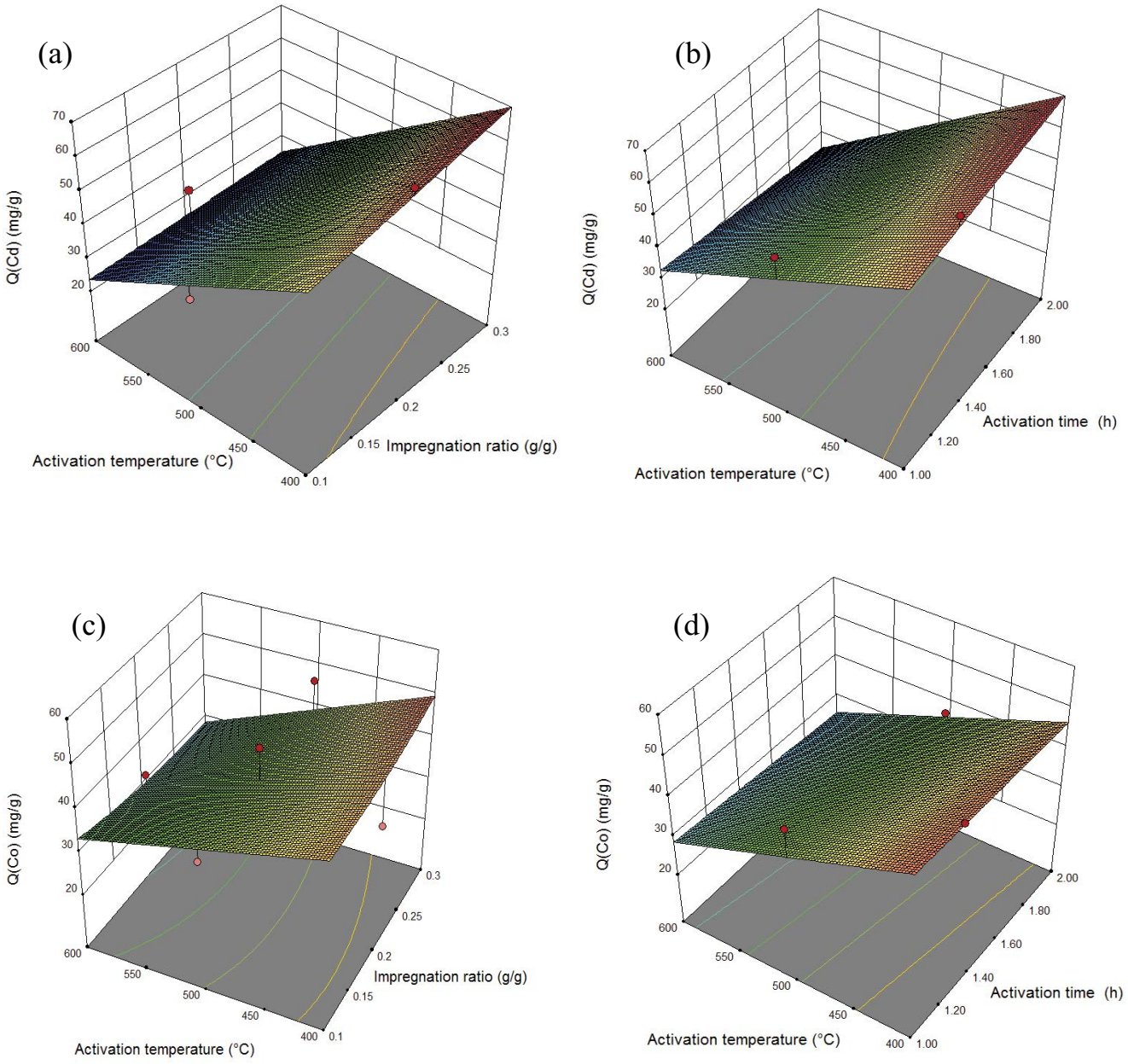

Fig. 2. Surface response plot for Cd(II) removal (a, b) and for Co(II) removal (c, d).

temperature of 400°C regardless of the impregnation ratio. For Figs. 2(b) and (d), it could be seen that cadmium and cobalt ions sorption increased with the decrease of the activation temperature, when the activation time is varied between 1 and 2 h, with a fixed impregnation ratio at 0.3 g/g for the removal of both metals. A high value of metal ions removal is observed at activation temperature of 400°C regardless of the activation time.

3.1.5. Normal probability plot of residuals

The normal probability plot of residuals for responses Y_1, Y_2, Y_3, and Y_4 are shown in Fig. 3. It can be seen in the figure that most of the data points were well distributed near to the straight line, which suggested an excellent relationship between experimental and predicted values of the responses [38]. Thus, all these statistical tests showed that quadratic models developed were proved to be successful in capturing the correlation between the process of variables and responses.

3.1.6. Optimization

The optimization of the process for studied responses was generated by the numerical optimization technique following desirability function. In this approach, the optimization of

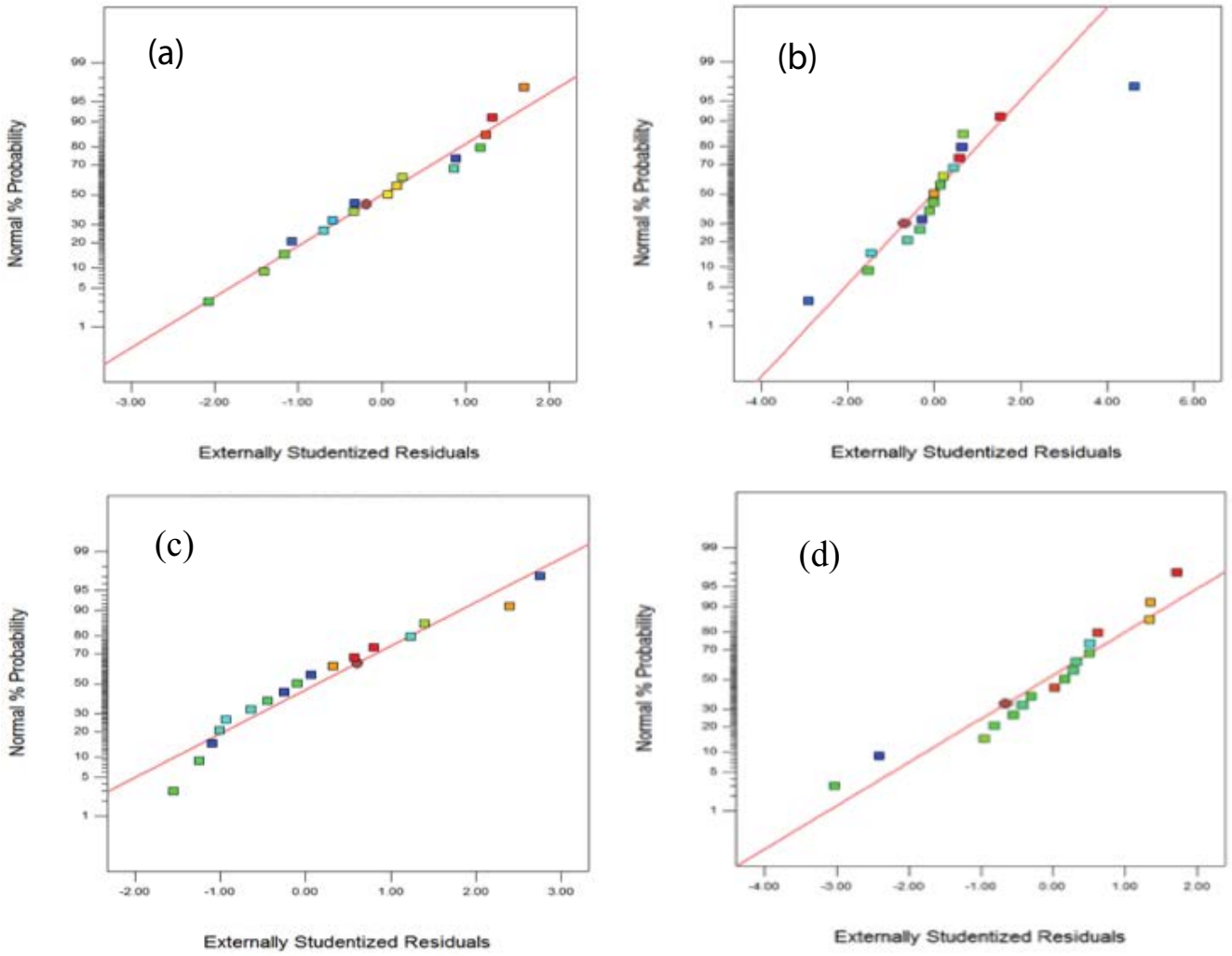

Fig. 3. Normal probability plots of residuals for the four responses: (a) iodine number, (b) MB index, (c) Cd(II), and (d) Co(II) removal capacities.

all responses simultaneously is possible by combining them into a single objective function, which basically represents the relationship of all responses that are to be optimized [39]. The maximum value of desirability function for these four responses was 1.000. It was obtained at activation temperature of 500°C, an activation time of 2 h, and an impregnation ratio of 0.2 g/g. Under these conditions, predicted values for IN, MB index, Cd(II) and Co(II) were 716.07 ± 55.41, 220.69 ± 29.93, 44.44 ± 5.90, and 36.70 ± 6.31 mg/g, respectively. These optimum values were checked experimentally which resulted in a deviation lower than 5%. The good correlation between these results indicates that Box–Behnken design along with desirability function could be successfully used to optimize the studied process.

Moreover, maximum IN and MB index were 822.5 and 285.4 mg/g, respectively. So, the best sorption of cadmium and cobalt were 67.69 and 51.64 mg/g, respectively. For the commercial activated carbon, those characteristics were 1,115.7 mg/g for IN, 288.9 mg/g for MB index, 0.8 mg/g for cadmium removal, 21.2 mg/g for cobalt removal.

3.2. Characterization of activated carbons prepared under optimum conditions

3.2.1. FTIR analysis of the adsorbents

The 4,000–400 cm^{-1} infrared spectral regions of chosen AC-KOH samples are presented in Fig. 4. The overall shapes of the spectra are very similar. The broad peaks around 3,300–3,400 cm^{-1} in the spectra were due to the stretching vibrations of the O–H bonds of water molecules which were adsorbed onto the surface of activated carbon [40]. The band around 1,710 cm^{-1} is usually caused by the stretching vibration of C=O in ketones, aldehydes, lactones, and carboxyl groups. The appearance of band in the region between 1,500 and 1,600 cm^{-1} indicate the presence of C=C bonds of aromatic compounds, this band increases with increasing impregnation ratio [41]. Moreover, the bands between 700 and 500 cm^{-1} are attributed to the out of plane deformation mode of the C–H bond in differently substituted aromatic rings.

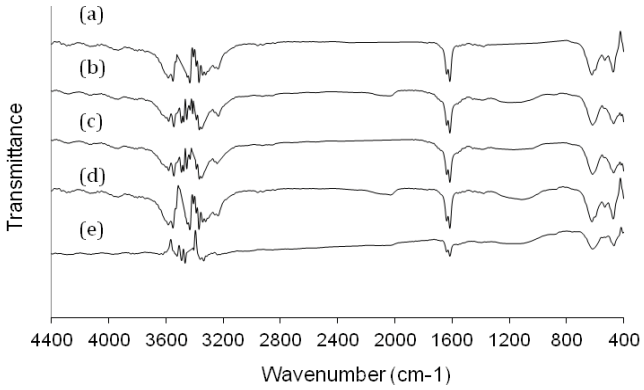

Fig. 4. FTIR spectra of (a) 0.1 g/g – 1 h 30 – 400, (b) 0.3 g/g – 1 h 30 – 400, (c) 0.2 g/g – 1 h 30 – 400, (d) 0.1 g/g – 1 h 30 – 600, and (e) 0.3 g/g – 1 h 30 – 600 activated carbons.

3.2.2. Boehm titration and point of zero charge of the adsorbents

The results of Boehm titrations for the chosen activated carbon samples are shown in Table 5. These results showed that all types of activated carbons contained significant amounts of acid groups than basic groups, which indicated that these activated carbons prepared had an acidic character. Then, the one's with the impregnation ratio of 0.1 g/g contained mainly phenolic groups followed by lactonic and carboxylic groups explaining their acidic character. Increasing the impregnation ratio to 0.3 g/g gave an active charcoal having a very large amount of lactone groups, carboxylic groups, and phenolic groups.

Values of pH_{PZC} presented in Table 1 were compatible with the conclusion extracted from data of oxygen functional groups whereby all samples displayed values near neutral showing little differences. The latter could be attributed to differences noted between acidic and basic sites.

3.3. Discussion

The use of KOH as activating agent has been shown to be effective in the production of activated carbon with a narrow pore distribution and well-developed porosity [42,43]. KOH was decomposed into potassium during the activation process. At higher activation temperature, the vaporized potassium would diffuse into the carbon layer to form pores in activated carbon. Based on researchers' results, the formation of pores in carbon by KOH activation was related to series of chemical reactions and K intercalation. The development of porosity is associated with gasification according to the following reaction [44]:

$$6KOH + 2C \rightarrow 2K + 3H_2 + 2K_2CO_3 \quad (7)$$

Correspondingly, K_2CO_3 was reduced by carbon to form K, K_2O, CO, and CO_2 according to following reactions [45]:

$$K_2CO_3 + 2C \rightarrow 2K + 3CO \quad (8)$$

$$K_2CO_3 \rightarrow K_2O + CO_2 \quad (9)$$

$$K_2O + 2C \rightarrow 2K + CO \quad (10)$$

It was assumed that metallic potassium formed during the gasification process would diffuse into the internal structure of carbon matrix widening existing pores and created new porosities. Pore widening normally begins, when there are a number of opened pores in the structure, therefore, it starts to be significant when the chemical ratio is reasonable. By increasing the KOH ratio in the low regime, more and more carbon atoms are oxidized, leading to an increase of both micropore and mesopore, and the surface area increases accordingly.

Moreover, the high mesoporosity of activated carbon samples was obtained during activation temperature of 500°C with an impregnation ratio of 0.2 g/g during activation time of 2 h. Nevertheless, the greater microporosity was obtained at the same conditions during impregnation ratio of 0.1 g/g. The adsorption capacity of cadmium onto AC samples was maximal (67.69 mg/g) with an activation temperature of 400°C and impregnation ratio of 0.3 g/g at 1.5 h of activation. Afterwards, the greater capacity of cobalt removal was 51.64 mg/g. It was obtained at same conditions during impregnation ratio of 0.1 g/g. The contour plots indicate that improvement of removal efficiencies for both heavy metals can be attributed to the increase of activation temperature and a lower impregnation ratio (0.1 g/g) for Cd(II) removal and a higher impregnation ratio (0.3 g/g) for Co(II) removal. The activation was also dependent on the activation time, which was best at 1.5 h. While, when the activation temperature and activation time increased, it could allow the degradation of

Table 5
Chemical groups on the surface and pH_{PZC} of the activated carbons

Activated carbon	Carboxylic groups (meq/g)	Lactonic groups (meq/g)	Phenolic groups (meq/g)	Total acid groups (meq/g)	Total basic groups (meq/g)	pH_{PZC}
0.1 g/g – 1 h 30 – 400°C	0.4012	0.4017	0.4029	1.2058	0.4008	6.75
0.3 g/g – 1 h 30 – 400°C	0.4004	0.4007	0.4003	1.2014	0.4016	6.66
0.2 g/g – 1 h 30 – 400°C	0.4008	0.4016	0.4012	1.2036	0.4025	6.28
0.1 g/g – 1 h 30 – 600°C	0.4017	0.4033	0.4048	1.2098	0.4004	6.81
0.3 g/g – 1 h 30 – 600°C	0.4010	0.4030	0.4033	1.2073	0.4011	6.93

the activated carbon sample and consequently, many pores and active sites were destroyed. It maybe was the reason of the reduction of both heavy metals removal.

Therefore, the sorption of these cationic metals could be due to their interactions with acidic functional groups found on the surface of indicated activated carbons. In fact, H^+ ions reacted with anionic functional groups on the surface of AC and they were resulted in the reduction of number of binding sites available for the adsorption of Cd(II) and Co(II). This increase could have been an effect on the presence of negative charge on the surface of the prepared activated carbon. These groups could be responsible for the metal binding because solution pH may also affect the charge of AC surfaces.

3.4. Sorption isotherm modeling

After the determination of optimal conditions for the preparation of an activated carbon having a greater capacity to remove heavy metal ions. Two activated carbons were chosen, the first one was activated at 400°C during 1.5 h with an impregnation ratio of 0.3 g/g, and the second one was activated at 400°C during 1.5 h with an impregnation ratio of 0.1 g/g. These samples were considered as optimized activated carbons for studding the isotherm models of cadmium and cobalt ions sorption.

In this investigation, the Langmuir and Freundlich isotherm equations were adopted to determine the equilibrium absorption (q_e, C_e) of Cd(II) and Co(II) on the optimized activated carbons.

Langmuir isotherm assumes that adsorption is limited to the formation of monolayer coverage of adsorbate on homogeneous adsorbent surface. It is assumed that once the adsorbent site is covered with the ions metal no further adsorption occurs at that site. It also suggests that all the adsorption sites are of equivalent energy [46]. This model can be applied successfully in many monolayer adsorption processes. The Langmuir equation is stated as follows:

$$q_e = \frac{q_m K_L C_e}{1 + K_L C_e} \tag{11}$$

where q_m (mg/g) is the maximum monolayer biosorption capacity, K_L (L/mg) is the Langmuir equilibrium constant related to the biosorption affinity, and C_e is the equilibrium concentration.

The Freundlich adsorption isotherm is an empirical equation employed to describe multilayer adsorption on a heterogeneous adsorption surface containing unequally available sites of different adsorption energies [47]. It is given as follows:

$$q_e = K_F C_e^{1/n} \tag{12}$$

where K_F ($mg^{1-1/n}/g/L^n$) is the Freundlich constant and n is the heterogeneity factor. The K_F value is related to the biosorption capacity; while $1/n$ value is related to the biosorption intensity.

In general $n > 1$ illustrates that adsorbate is favorably adsorbed on an adsorbent, and corresponds to a normal an L-type Langmuir isotherm. The higher the n value, the stronger the adsorption intensity.

The obtained sorption isotherms parameters are summarized in Table 6 and Fig. 5. According to the correlation coefficient, the experimental results showed better correlation at Langmuir isotherm model with high value of the r^2, which is in order of 0.99. As shown, the maximum adsorption capacity (q_m) is 90.58 mg/g for cadmium removal and 70.16 mg/g for cobalt sorption, onto carbon activated at 400°C during 1.5 h with an impregnation ratio of 0.3 g/g and the carbon activated at 400°C during 1.5 h with an impregnation ratio of 0.1 g/g, respectively. These capacities assume a monolayer sorption processes for cobalt and cadmium.

While, the AC activated at 400°C during 1.5 h with an impregnation ratio of 0.3 g/g has a greater sorption efficiency of cadmium than the AC prepares in the same condition of the preceding one but with an impregnation ratio of 0.1 g/g. Furthermore, the CA activated at 400°C during 1.5 h with an impregnation ratio of 0.1 g/g, the activated carbon presents a higher sorption of cobalt ions. We can conclude that both the optimized activated carbons are more able to adsorb cadmium than cobalt ions.

The maximum Langmuir sorption capacities mentioned earlier were compared with previous studies onto various activated carbons with different preparation

Table 6
Isotherm parameters for the sorption of Cd(II) and Co(II) of AC-0.3 g/g – 1 h 30 – 400°C and AC-0.1 g/g – 1 h 30 – 400°C

Isotherms	Parameters	0.3 g/g – 1 h 30 – 400°C		0.1 g/g – 1 h 30 – 400°C	
		Cd(II)	Co(II)	Cd(II)	Co(II)
Langmuir	q_m (mg/g)	90.58	74.01	82.08	77.24
	K_L (L/mg)	0.104	0.035	0.071	0.048
	r^2	0.999	0.997	0.998	0.992
Freundlich	n	7.479	4.087	6.225	5.101
	K_F ($mg^{1-1/n}/g/L^n$)	44.66	18.48	34.19	25.69
	r^2	0.997	0.995	0.996	0.987

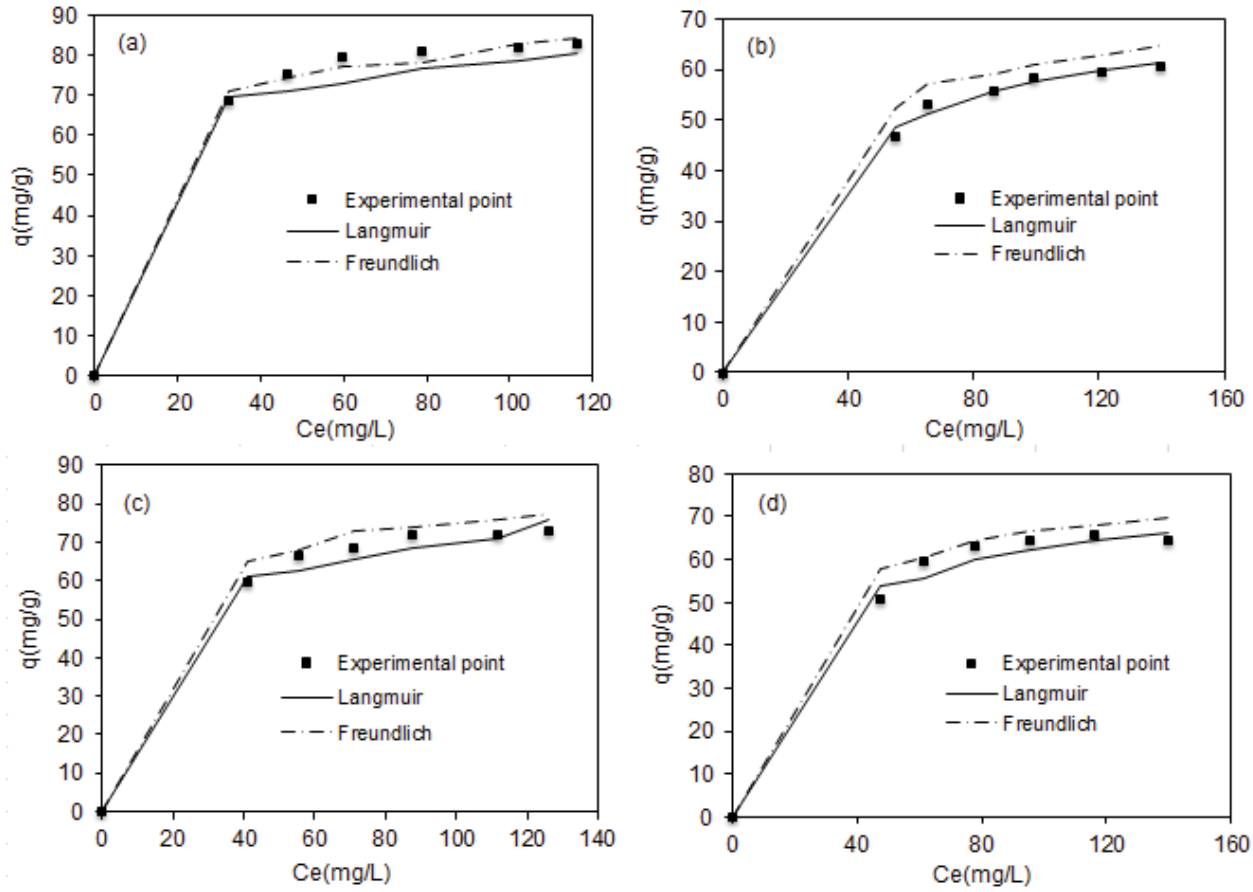

Fig. 5. Experimental points (R = 1 g/L, pH = 6.50, t = 2 h, T = 25°) and nonlinear fitted curve isotherms: Cd(II) onto AC-0.3 g/g – 1 h 30 – 400°C (a), Co(II) onto 0.3 g/g – 1 h 30 – 400°C (b), Cd(II) onto 0.1 g/g – 1 h 30 – 400°C (c), and Co(II) onto 0.1 g/g – 1 h 30 – 400°C (d).

Table 7
Adsorption capacities (mg/g) for activated carbons

Activated carbon	Activating agent	Cd(II)	Co(II)	References
Activated biochar	NaOH	167.3	–	[48]
Activated carbon derived from bagasse	H_3PO_4	38.0	–	[49]
Silkworms' feces-based activated carbons	$TiCl_4$	62.89	–	[50]
Olive stone activated carbon	KOH	11.72	–	[51]
Olive stone activated carbon	$ZnCl_2$	1.85	–	[52]
Activated carbon was nut shells	H_3PO_4	104.17	–	[53]
Spartina alterniflora activated carbon	H_3PO_4	47.58	–	[54]
Apricot stone activated carbon	H_3PO_4	–	111.11	[55]
Activated potato peels (PoP400 at 25°C)	H_3PO_4	–	373.00	[56]
Activated potato peels (PoP600 at 25°C)	H_3PO_4	–	405.00	[56]
Bagasse pith activated carbon	$H_2S + SO_2$	–	153.60	[57]
Leaves of *Acacia nilotica*	H_2SO_4	–	35.46	[58]
Activated *Glebionis coronaria* L. (AC-500°C/400°C/1 h/2 g/g	KOH	115.99	44.85	[28]
Activated *Glebionis coronaria* L. (AC 600°C/500°C/1 h/2 g/g)	KOH	106.93	46.80	[28]
Activated *Glebionis coronaria* L. (AC-600°C/400°C/1 h/1.5 g/g)	H_3PO_4	118.78	42.86	[59]
Activated *Diplotaxis harra* (AC-500°C/400°C/1 h/1.5 g/g)	H_3PO_4	62.58	82.55	[60]
Activated *Diplotaxis harra* (AC-500°C/400°C/1 h/2 g/g)	H_3PO_4	51.83	69.86	[60]
Activated carob shell (AC-0.3 g/g – 1 h 30 – 400°C)	KOH	90.58	–	This study
Activated carob shell (AC-0.1 g/g – 1 h 30 – 400°C)	KOH	–	70.16	This study

conditions cited in the literature (Table 7). It could be seen that the experimental data in this study are higher than the most prepared activated carbons using cadmium and cobalt sorption in the literature.

4. Conclusion

This work investigated the feasibility of preparing activated carbons from carob shell biomass for the removal of heavy metals. The KOH activation was successful, allowed an effective activated carbon with a high sorption capacity of Cd(II) and Co(II). The Box–Behnken design and response surface methodology were applied to determine the best preparation conditions and the greater heavy metals removal. Three different factors, including impregnation ratio, activation time, and activation temperature, are chosen. The obtained results indicated that the most influential factors on the IN are the impregnation ratio, activation temperature, and the interaction between impregnation ratio and activation time with negative impact. For MB index the influential factors are the impregnation ratio, activation temperature with negative impact, and activation time with a positive impact. While, the factors influenced the cadmium and cobalt removal are the activation temperature and the interaction between activation time and activation temperature with negative impact. Furthermore, the greater value of cadmium removal was obtained at an impregnation ratio of 0.3 g/g, activation time of 1.5 h, and an activation temperature of 400°C. However, the best value for cobalt removal was obtained at an impregnation ratio of 0.1 g/g, an activation time of 1.5 h, and activation temperature of 400°C. At these optimal conditions, the maximum IN and MB index were 822.5 and 285.4 mg/g, respectively. On the other hand, the maximum sorption capacities obtained with the application of the Langmuir isotherm model are 90.58 and 82.08 mg/g for cadmium sorption and 74.01 and 77.24 mg/g for cobalt sorption.

References

[1] L. Juan, L. Xuwen, W. Jin, X. Tangfu, Y. Meiling, B.N. Stanley, L. Holger, K. Lingjun, X. Enzhong, B. Zhian, L. Nuo, C. Yongheng, L. Wensheng, Provenance of uranium in a sediment core from a natural reservoir, South China: application of Pb stable isotope analysis, Chemosphere, 193 (2018) 1172–1180.

[2] J. Liu, X. Luo, J. Wang, T. Xiao, D. Chen, G. Sheng, M. Yin, H. Lippold, C. Wang, Y. Chen, Thallium contamination in arable soils and vegetables around a steel plant-a newly-found significant source of Tl pollution in South China, Environ. Pollut., 224 (2017) 445–453.

[3] C.S. Ezeonu, R. Tagbo, E.N. Anike, O.A. Oje, I.N.E. Onwurah, Biotechnological tools for environmental sustainability: prospects and challenges for environments in Nigeria—A standard review, Biotechnol. Res. Int., 450802 (2012) .

[4] M.F. Hamoda, I. Al-Ghusain, N.Z. Al-Mutairi, Sand filtration of wastewater for tertiary treatment and water reuse, Desalination, 164 (2004) 203–211.

[5] V. Innocenzi, F. Veglio, Separation of manganese, zinc and nickel from leaching solution of nickel-metal hydride spent batteries by solvent extraction, Hydrometallurgy, 129–130 (2012) 50–58.

[6] A. Dirany, I. Sires, N. Oturan, A. Ozcan, M. Oturan, Electrochemical treatment of the antibiotic sulfachloropyridazine: kinetics, reaction pathways, and toxicity evolution, Environ. Sci. Technol., 46 (2012) 4074–4082.

[7] M.J. Gonzalez-Munoz, M.A. Rodriguez, M. Luque, J.R. Alvarez, Recovery of heavy metals from metal industry waste waters by chemical precipitation and nanofiltration, Desalination, 200 (2006) 742–744.

[8] R. Kiefer, A.I. Kalinitchev, W.H. Holl, Column performance of ion exchange resins with aminophosphonate functional groups for elimination of heavy metals, React. Funct. Polym., 67 (2007) 1421–1432.

[9] J. Shen, A. Schäfer, Removal of fluoride and uranium by nanofiltration and reverse osmosis: a review, Chemosphere, 117 (2014) 679–691.

[10] N. Barka, K. Ouzaouit, S. Qourzal, A. Assabbane, M. Abdennouri, M. El Makhfouk, A. Nounah, Y. Ait-Ichou. Kinetics and equilibrium of cadmium removal from aqueous solutions by sorption onto synthesized hydroxyapatite, Desal. Wat. Treat., 43 (2012) 8–16.

[11] W. Linghu, H. Yang, Y. Sun, G. Sheng, Y. Huang, One-pot synthesis of LDH/GO composites as highly effective adsorbents for decontamination of U(VI), ACS Sustainable Chem. Eng., 5 (2017) 5608–5616.

[12] P. Rajasulochana, V. Preethy, Comparison on efficiency of various techniques in treatment of waste and sewage water – a comprehensive review, Resour. Efficient Technol., 2 (2016) 175–184.

[13] G. Sheng, C. Huang, G. Chen, J. Sheng, X. Ren, B. Hu, J. Ma, X. Wang, Y. Huang, A. Alsaedi, T. Hayat, Adsorption and co-adsorption of graphene oxide and Ni(II) on iron oxides: a spectroscopic and microscopic investigation, Environ. Pollut., 233 (2018) 125–131.

[14] B. Hu, F. Ye, X. Ren, D. Zhao, G. Sheng, H. Li, J. Ma, X. Wang, Y. Huang, X-ray absorption fine structure study of enhanced sequestration of U(VI) and Se(IV) by montmorillonite decorated zero valent iron nanoparticles, Environ. Sci. Nano, 3 (2016) 1460–1472.

[15] B. Hu, G. Chen, C. Jin, J. Hu, C. Huang, J. Sheng, G. Sheng, J. Ma, Y. Huang, Macroscopic and spectroscopic studies of the enhanced scavenging of Cr(VI) and Se(VI) from water by titanate nanotube anchored nanoscale zero-valent iron, J. Hazard. Mater., 336 (2017) 214–221.

[16] B.W. Hu, C.C. Huang, X. Li, G.D. Sheng, H. Li, X.M. Ren, J.Y. Ma, J. Wang, Y.Y. Huang, Macroscopic and spectroscopic insights into the mutual interaction of graphene oxide, Cu(II), and Mg/Al layered double hydroxides, Chem. Eng. J., 313 (2017) 527–534.

[17] Q. Fu, X. Zhou, L. Xu, B. Hu, Fulvic acid decorated Fe_3O_4 magnetic nanocomposites for the highly efficient sequestration of Ni(II) from aqueous solution, J. Mol. Liq., 208 (2015) 92–98.

[18] B. Hu, Q. Hu, D. Xu, C. Chen, Macroscopic and microscopic investigation on adsorption of Sr(II) on sericite, J. Mol. Liq., 225 (2017) 563–568.

[19] S.L. Gayatri, Md. Ahmaruzzaman, Adsorption technique for the removal of phenolic compounds from wastewater using low-cost natural adsorbents, Phys. Sci. Technol., 5 (2010) 156–166.

[20] K.M. Doke, E.M. Khan, Equilibrium, kinetic and diffusion mechanism of Cr(VI) adsorption onto activated carbon derived from wood apple shell, Arabian J. Chem., 10 (2017) S252–S260.

[21] S. Larous, A.H. Meniai, Adsorption of Diclofenac from aqueous solution using activated carbon prepared from olive stones, Int. J. Hydrogen Energy, 41 (2016) 10380–10390.

[22] A.M.M. Vargas, C.A. Garcia, E.M. Reis, E. Lenzi, W.F. Costa, V.C. Almeida, NaOH-activated carbon from flamboyant (*Delonix regia*) pods: optimization of preparation conditions using central composite rotatable design, Chem. Eng. J., 162 (2010) 43–50.

[23] D. Savova, E. Apak, E. Ekinci, F. Yardım, N. Petrov, T. Budinova, M. Razvigorova, V. Minkova, Biomass conversion to carbon adsorbents and gas, Biomass Bioenergy, 21 (2001) 133–142.

[24] H.M. Mozammel, O. Masahiro, S.C. Bahattacharya, Activated charcoal from coconut shell using $ZnCl_2$ activation, Biomass Bioenergy, 22 (2002) 397–400.

[25] W. Heschel, E. Klose, On the suitability of agricultural by-products for the manufacture of granular activated carbon, Fuel, 74 (1995) 1786–1791.

[26] L. Dong, J. Yang, Y. Mou, G. Sheng, L. Wang, W. Linghu, A.M. Asiri, K.A. Alamry, Effect of various environmental factors on the adsorption of U(VI) onto biochar derived from rice straw, J. Radioanal. Nucl. Chem., 314 (2017) 377–386.
[27] H. Tounsadi, A. Khalidi, M. Abdennouri, N. Barka, Activated carbon from *Diplotaxis harra* biomass: optimization of preparation conditions and heavy metal removal, J. Taiwan Inst. Chem. Eng., 59 (2016) 348–358.
[28] H. Tounsadi, A. Khalidi, M. Farnane, M. Abdennouri, N. Barka, Experimental design for the optimization of preparation conditions of highly efficient activated carbon from *Glebionis coronaria* L. and heavy metals removal ability, Process Saf. Environ. Prot., 102 (2016) 710–723.
[29] M. Xu, Q. Huang, R. Sunab, X. Wang, Simultaneously obtaining fluorescent carbon dots and porous active carbon for supercapacitors from biomass, RSC Adv., 6 (2016) 88674–88682.
[30] B. Hu, Q. Hu, D. Xu, C. Chen, The adsorption of U(VI) on carbonaceous nanofibers: a combined batch, EXAFS and modeling techniques, Sep. Purif. Technol., 175 (2017) 140–146.
[31] B.W. Hu, Q.Y. Hu, C.G. Chen, Y.B. Sun, D. Xu, G.D. Sheng, New insights into Th(IV) speciation on sepiolite: evidence for EXAFS and modeling investigation, Chem. Eng. J., 322 (2017) 66–72.
[32] W. Linghu, Y. Sun, H. Yang, K. Chang, J. Ma, Y. Huang, W. Dong, A. Alsaedi, T. Hayat, Sorption of U(VI) on magnetic sepiolite investigated by batch and XANES techniques, J. Radioanal. Nucl. Chem., 314 (2017) 1825–1832.
[33] H.P. Boehm, Surface oxides on carbon and their analysis: a critical assessment, Carbon, 40 (2002) 145–149.
[34] J.S. Noh, J.A. Schwarz, Estimation of the point of zero charge of simple oxides by mass titration, J. Colloid Interface Sci., 130 (1989) 157–164.
[35] C. Elliott, T. Colby, H. Iticks, Activated carbon obliterans alter aspiration of activated charcoal, Chest J., 96 (1989) 672–674.
[36] M. Khajeh, M. Kaykhaii, A. Sharafi, Application of PSO-artificial neural network and response surface methodology for removal of methylene blue using silver nanoparticles from water samples, J. Ind. Eng. Chem., 19 (2013) 1624–1630.
[37] M. Khajeh, M. Gharan, Separation of organic acid compounds from biological samples by zinc oxide nanoparticles–chitosan using genetic algorithm based on response surface methodology and artificial neural network, J. Chemom., 28 (2014) 539–547.
[38] J. Antony, Design of Experiments for Engineers and Scientists, Butterworth-Heinemann, New York, 2003.
[39] C.S. Aksezer, On the sensitivity of desirability functions for multiresponse optimization, J. Ind. Manage. Optim., 4 (2008) 685–696.
[40] F. Adam, A. Iqbal, The oxidation of styrene by chromium–silica heterogeneous catalyst prepared from rice husk, Chem. Eng. J., 160 (2010) 742–750.
[41] C.F. Hsu, L. Zhang, H. Peng, J. Travas-Sejdic, P.A. Kilmartin, Structural changes in polyaniline upon reaction with DPPH, Curr. Appl. Phys., 8 (2008) 316–319.
[42] L. Khezami, A. Ould-Dris, R. Capart, Activated carbon from thermo-compressed wood and other lignocellulosic precursors, Bioresources, 2 (2007) 193–209.
[43] T. Kawano, M. Kubota, M.S. Onyango, F. Watanabe, H. Matsuda, Preparation of activated carbon from petroleum coke by KOH chemical activation for adsorption heat pump, Appl. Therm. Eng., 28 (2008) 865–871.
[44] A.H. Basta, V. Fierro, H. El-Saied, A. Celzard, 2-steps KOH activation of rice straw: an efficient method for preparing high performance activated carbons, Bioresour. Technol., 100 (2009) 3941–3947.
[45] D.W. McKee, Mechanisms of the alkali metal catalyzed gasification of carbon, Fuel, 62 (1983) 170–175.
[46] I. Langmuir, The constitution and fundamental properties of solids and liquids, J. Am. Chem. Soc., 38 (1916) 2221–2295.
[47] H. Freundlich, W. Heller, The adsorption of cis- and trans-azobenzene, J. Am. Chem. Soc., 61 (1939) 2228–2230.
[48] C.M. Park, J. Han, K.H. Chu, Y.A.J. Al-Hamadani, N. Her, J. Heo, Y. Yoon, Influence of solution pH, ionic strength, and humic acid on cadmium adsorption onto activated biochar: experiment and modelling, J. Ind. Eng. Chem., 48 (2017) 186–193.
[49] D. Mohan, K.P. Singh, Single- and multi-component adsorption of cadmium and zinc using activated carbon derived from bagasse Fan agricultural waste, Water Res., 36 (2002) 2304–2318.
[50] G.M.S. El Shafei, I.M.A. ElSherbiny, A.S. Darwish, C.A. Philip, Silkworms' feces-based activated carbons as cheap adsorbents for removal of cadmium and methylene blue from aqueous solutions, Chem. Eng. Res. Des., 92 (2014) 461–470.
[51] T.M. Alslaibi, I. Abustan, M.A. Ahmad, A. Abu Foul, Cadmium removal from aqueous solution using microwaved olive stone activated carbon, J. Environ. Chem. Eng., 1 (2013) 589–599.
[52] I. Kula, M. Ugurlu, H. Karaoglu, A. Celik, Adsorption of Cd(II) ions from aqueous solutions using activated carbon prepared from olive stone by $ZnCl_2$ activation, Bioresour. Technol., 99 (2008) 492–501.
[53] A.F. Tajar, T. Kaghazchi, M. Soleimani, Adsorption of cadmium from aqueous solutions on sulfurized activated carbon prepared from nut shells, J. Hazard. Mater., 165 (2009) 1159–1164.
[54] Z. Wang, E. Nie, J. Li, Y. Zhao, X. Luo, Z. Zheng, Carbons prepared from *Spartina alterniflora* and its anaerobically digested residue by H_3PO_4 activation: characterization and adsorption of cadmium from aqueous solutions, J. Hazard. Mater., 188 (2011) 29–36.
[55] M. Abbas, S. Kaddour, M. Trari, Kinetic and equilibrium studies of cobalt adsorption on apricot stone activated carbon, J. Ind. Eng. Chem., 20 (2014) 745–751.
[56] G.Z. Kyzas, E.A. Deliyanni, K.A. Matis, Activated carbons produced by pyrolysis of waste potato peels: cobalt ions removal by adsorption, Colloids Surf., A, 490 (2016) 74–83.
[57] K.A. Krishnan, T.S. Anirudhan, Kinetic and equilibrium modelling of cobalt(II) adsorption onto bagasse pith based sulphurised activated carbon, Chem. Eng. J., 137 (2008) 257–264.
[58] P. Thilagavathy, T. Santhi, Kinetics, Isotherms and equilibrium study of Co(II) adsorption from single and binary aqueous solutions by *Acacia nilotica* leaf carbon, Chinese J. Chem. Eng., 22 (2014) 1193–1198.
[59] H. Tounsadi, A. Khalidi, A. Machrouhi, M. Farnane, R. Elmoubarki, A. Elhalil, M. Sadiq, N. Barka, Highly efficient activated carbon from *Glebionis coronaria* L. biomass: optimization of preparation conditions and heavy metals removal using experimental design approach, J. Environ. Chem. Eng., 4 (2016) 4549–4564.
[60] H. Tounsadi, A. Khalidi, M. Farnane, A. Machrouhi, A. Elhalil, N. Barka, Adsorptive removal of heavy metals from aqueous solution using chemically activated *Diplotaxis harra* biomass, Surf. Interfaces, 4 (2016) 84–94.